Use of a biomimetic strategy to engineer bone

C. E. Holy,[1] J. A. Fialkov,[2] J. E. Davies,[1,3,4] M. S. Shoichet[1,4]
[1]*Institute for Biomaterials and Biomedical Engineering, University of Toronto, 4 Taddle Creek Road, Toronto, Ontario, Canada M5S 3G9*
[2]*Sunnybrook and Women's College Health Sciences Centre, University of Toronto, 2075 Bayview Avenue, North York, Ontario, Canada M4N 3M5*
[3]*Faculty of Dentistry, University of Toronto, 124 Edward Street, Toronto, Ontario, Canada M5G 1G6*
[4]*Department of Chemical Engineering and Applied Chemistry, Department of Chemistry, University of Toronto, 200 College Street, Toronto, Ontario, Canada M5S 3E5*

Received 20 May 2002; accepted 3 June 2002

Abstract: Engineering trabecular-like, three-dimensional bone tissue throughout biodegradable polymer scaffolds is a significant challenge. Using a novel processing technique, we have created a biodegradable scaffold with geometry similar to that of trabecular bone. When seeded with bone-marrow cells, new bone tissue, the geometry of which reflected that of the scaffold, was evident throughout the scaffold volume and to a depth of 10 mm. Preseeded scaffolds implanted in non-healing rabbit segmental bone defects allowed new functional bone formation and bony union to be achieved throughout the defects within 8 weeks. This marks the first report of successful three-dimensional bone-tissue engineering repair using autologous marrow cells without the use of supplementary growth factors. We attribute our success to the novel scaffold morphology. © 2003 Wiley Periodicals, Inc. J Biomed Mater Res 65A: 447–453, 2003

Key words: tissue engineering; regenerative medicine; bone defect repair; scaffold; poly(lactic-*co*-glycolic acid)

INTRODUCTION

Bone-tissue engineering aims to heal bone defects with autologous cells and tissue without the donor site morbidity and expense associated with harvesting autogenous bone. One such strategy involves seeding autologous osteogenic cells *in vitro* throughout a biodegradable scaffold to create a scaffold–cell hybrid that may be called a tissue engineering construct (TEC). This strategy for bone regeneration is distinctly different from those that do not employ the seeding of autologous osteogenic cells but rely on stabilization of the hematoma at the operative site,[1] and from others that rely on the employment of recombinant growth factors.[2]

The main challenge in preparing a useful TEC is to obtain a ubiquitous distribution of cells, and hence new tissue, throughout the entire 3-dimensional scaffold volume. The morphology of some biodegradable polymer scaffolds, due to insufficient interconnected macroporosity, has been shown to limit cell colonization, and thus new tissue formation, to the superficial pore layer, resulting in tissue only ≈200 μm thick.[3–5]

Porous organic cements also have been used to fill bone-defect sites in rodents; however, new bone-tissue formation has not been demonstrated either *in vitro* or *in vivo* in segmental critical-size defects.[6] Other strategies using inorganic scaffolds of calcium phosphate have allowed cell and tissue formation throughout the entire volume of the scaffolds,[7,8] but the inorganic material itself remains in the implantation site long after bone repair.

We report herein a novel processing technology for creating a biodegradable polymer scaffold that mimics the architecture of trabecular bone and that supports bone growth throughout its volume both *in vitro* and *in vivo*. The scaffolds were prepared with poly(lactide-co-glycolide) (PLGA), a polymer commonly used for

Correspondence to: M. S. Shoichet, Institute for Biomaterials and Biomedical Engineering; e-mail: molly@ecf. utoronto.ca; or J.E. Davies, Institute for Biomaterials and Biomedical Engineering; e-mail: davies@ecf.utoronto.ca

Contract grant sponsor: Canadian Institutes of Health Research (formerly the Medical Research Council of Canada)
Contract grant sponsor: The Ontario Research and Development Challenge Fund
Contract grant sponsor: BoneTec Corporation
Contract grant sponsor: Physician's Services' Incorporated Foundation

sutures and previously shown to allow bone-marrow cell differentiation into osteoblasts *in vitro*[9] and to degrade on a time scale concomitant with that of bone formation *in vivo*.[10]

Building on the tissue-engineering principle, we envision that our scaffolds will be temporary, providing the appropriate geometry for cell colonization and tissue formation. Thus, in a fashion analogous to autologous trabecular bone grafting, we specifically have not focused on the inherent mechanical properties of the scaffold except for the necessity of supporting cell colonization and matrix formation, as we have reported elsewhere.[11] This approach was adopted not only because we envision that our scaffolds ultimately will be replaced by remodeling bone at the wound site, but also because autogenous trabecular bone chips, while providing mechanical support for the regenerating bone tissue, are not themselves implicated in the biomechanical loading of the operated bone.

MATERIALS AND METHODS

Scaffold formation

PLGA 75/25 (Birmingham Polymers, Inc. Birmingham, AL; Mw 81,500 g/mol) had an intrinsic viscosity of 0.87 dL/g at 30°C in chloroform. To a 1% PLGA solution in DMSO were added 2 g/mL of glucose crystals. The solution was frozen and immersed in H_2O and sugar was extracted from the precipitated polymer. The scaffolds were rinsed extensively in water to remove any residual solvent and then dried to constant mass (10 μm of Hg, 72h). The scaffolds were disinfected in 70% EtOH for 30 min prior to being seeded with cells for *in vitro* cell culture. For *in vivo* experiments, the scaffolds were sterilized by exposure to argon plasma (4 min at 100 W)[12] and then pre-wetted in ethanol prior to being seeded with cells and/or implanted.

Cell culture

First-passage primary bone-marrow-derived cells were seeded onto 0.25-cm^3 scaffolds using protocols and media described in detail elsewhere.[13,14] Briefly, bone-marrow-derived cells were collected from both femora of young male Wistar rats (approximately 120 g) and from both iliac crests of rabbits into a fully supplemented medium (FSM): α-MEM supplemented with 15% fetal bovine serum, 50 mg/mL of ascorbic acid, 10 m*M* of β-glycerophosphate and antibiotics (0.1 mg/mL of penicillin G, 0.05 mg/mL of gentamicin, and 0.3 mg/mL of fungizone); $10^{-8}M$ of dexamethasone (Dex) was added to the FSM of only Dex(+) cultures.

Cells were maintained in culture for 6 days and re-fed at days 2 and 5 with FSM. At day 6, Dex(−) cells were trypsinized with 0.01% trypsin in PBS whereas Dex(+) cultures, in which signs of calcification were visible, were trypsinized with 0.01% trypsin and 10 μ*M* of ethylene diamine tetraacetic acid (EDTA) in PBS. Dex(+) and Dex(−) cells then were seeded onto separate pre-wetted scaffolds at a concentration of 7.5×10^5 cells/scaffold. The rat cultures were maintained for 42 days at 37°C and 5% CO_2 and re-fed every 2–3 days with FSM. Rabbit cultures were implanted *in vivo* after 14 days in culture. Dex was added to the FSM of Dex(+) cell cultures at a concentration of $10^{-8}M$ at re-feeding.

Tetracycline/HCl powder (Sigma, St. Louis, MO) was dissolved in α-MEM to prepare a stock solution of 90 mg/mL. A new tetracycline containing fully supplemented medium (TFSM) was prepared of α-MEM containing 15% fetal bovine serum, 50 mg/mL ascorbic acid, 10 m*M* of β-glycerophosphate, and 9 mg/mL of tetracycline. The TFSM was used for the last re-feeding on day 40. At day 42, cultures were washed in α-MEM (10 times, ≈3 min each), and fixed overnight in Karnovsky's fixative (2.0% paraformaldehyde, 2.5% glutaraldehyde, and 0.1*M* of sodium cacodylate buffer, pH 7.2–7.4). A few cultures were kept for SEM observations and were dehydrated in a series of graded alcohol solutions (70%, 100%) and freeze-dried at 0.01 mm of Hg for 2 days. All other cultures were kept in 0.1*M* of cacodylate buffer for histologic observations.

Rabbit osteotomy

New Zealand white (NZW) rabbits (Riemans Fur Ranches Limited, St. Agatha, Ontario) were housed and cared for in accordance with the Canadian Council on Animal Care Guidelines. Animals were provided food and water *ad libitum*. An overnight (14 h) food and water deprivation period preceded the surgery. An induction mixture of Ketamine (Ketamine hydrochloride 50 mg/kg), Rompun (xylazine, 5 mg/kg), and acetylpromazine (0.75 mg/kg) was administered intramuscularly as an anesthetic. The lateral left limb of each rabbit was shaved and prepared with an antiseptic solution of 10% povidone–iodine. Strict sterile procedures were followed. The femur was exposed through lateral longitudinal incision. The periosteum was lifted using a periosteal elevator, and a 2.7-mm titanium, eight-hole linear reconstruction mandibular plate (Leibinger, Howmedica) was applied to the anterolateral cortex and fixed with six 2.7-mm bicortical screws, three on either side of the osteotomy. A 1.2-cm defect was sawed, and rabbit bone-marrow cell-cultured PLGA foams were implanted into the defects. The incisions were closed in two layers.

Scanning electron microscopy

Samples for SEM observation were sputter-coated with ≈10 nm of gold (Polaron Instrument Inc., Doylestown, PA). Scanning electron micrographs were taken on a Hitachi 2500 scanning electron microscope (SEM) at a 15-kV acceleration voltage.

Confocal microscopy

Samples were placed in custom-built chambers in 0.1*M* of cacodylate buffer. Fluorescent signals were detected by optical sectioning in a Bio-Rad MRC-600 confocal laser microscope.

Osteocalcin immunolabeling

Osteocalcin expression in both Dex(+) and Dex(−) cultures was assessed by immunohistochemical methods with a goat anti-rat osteocalcin antiserum (Biomedical Technologies Inc., Stoughton, MA) at a final dilution of 1:6000, followed by a second antibody labeling with donkey anti-goat IgG conjugated to horseradish peroxidase serum at a concentration of 1:250. The control was non-immune goat serum (1/1000 in buffer). A 3,3′-diaminobenzidine (DAB) substrate kit for peroxidase (Vector Laboratories, Burlingame, CA), supplemented with nickel chloride, was used to develop the staining.

Histology of *in vitro* samples

Fixed Dex(+) and Dex(−) cultured scaffolds were stained with hematoxylin and eosin *in situ*, embedded in Tissue-Tek, and cut into 10-μm thick sections at −20°C using an Ames Lab-tek cryostat (Elkhart, IN). Scaffold sections were further counterstained with von Kossa's silver nitrate stain for visualization of mineralized matrix. Histologic sections were examined by light microscopy (Leitz, Heerbrugg, Switzerland), and pictures were taken with 100 ASA Kodak film.

Histology of *in vivo* samples

Entire femurs were dissected and fixed in 10% formalin for 2 weeks. The bones then were dehydrated in graded ethanol solutions, defatted in xylene, and embedded in Osteobed™. The embedded bones then were halved longitudinally along the middle of the plate. Both sides were stained with Van Giesen and toluidine blue.

Radiographs

Radiographs of rabbit femurs were taken at $t = 0$, 2, 4, 6, and 8 weeks postoperatively. Serial radiographs were assessed for bone regeneration at each time point using a simple yes or no system ($n = 9$ per group and per time point).

RESULTS AND DISCUSSION

For the creation of our scaffolds, we used a new processing technique that combined extraction with phase inversion without the use of toxic solvents. The choice of PLGA for the scaffold was one of practicality and positive results. We have been able to apply our processing strategy to other polymers but have focused on PLGA due to its extensive use *in vivo* and its ability to support bone tissue. Rodent bone-marrow cells that were seeded onto our scaffolds grew and produced mineralized bone tissue throughout the entire scaffold volume, as documented by osteocalcin immunolabeling, histology, and tetracycline labeling. TECs preseeded with autologous lagomorph bone-marrow-derived cells also were implanted into a 1.2-cm segmental femoral defect in rabbits and demonstrated new bone formation *in vivo* throughout the entire critical-size defect.

Thus we successfully demonstrated 3-D bone tissue formation throughout scaffolds several millimeters thick both *in vitro* and *in vivo*. Although PLGA has been criticized for acidic degradation products that stimulate an inflammatory response,[15] we observed evidence of neither acidic degradation products in model degradation studies *in vitro*[10] nor an inflammatory response *in vivo*. While we do not dispute the mechanism of degradation nor the inflammatory responses observed by others, we believe that the macroporous geometry of our scaffolds allows facile diffusion of acidic products out of the scaffold, which further is assisted by the rapid invasion of host vascular tissue, thereby avoiding the concentrated acidic milieu and associated inflammatory response.

Biodegradable scaffolds were prepared from a random copolymer of poly(D,L-lactide-*co*-glycolide) containing 75% lactide and 25% glycolide (PLGA 75/25) in a process that yielded scaffolds with a morphology similar to that of trabecular bone, as shown in Figure 1(a,b). The resemblance between these synthetic scaffolds and trabecular bone was further observed by scanning electron microscopy [Fig. 1(c)].

In particular, the scaffold architecture provided large pore diameters, high porosity, and large interconnections between the pores that were separated by struts rather than by solid, membranous walls. We chose to create scaffolds with a morphology similar to that of trabecular bone because the open pore geometry of the natural tissue is thought both to enhance metabolic activity and to allow continuous and highly responsive bone remodeling.[16] While salt-extraction techniques result in highly porous scaffolds, the limited interconnectivity between the pores restricts cellular and particularly tissue penetration into the scaffold. Conversely, our scaffolds present a highly porous, interconnected morphology that facilitates

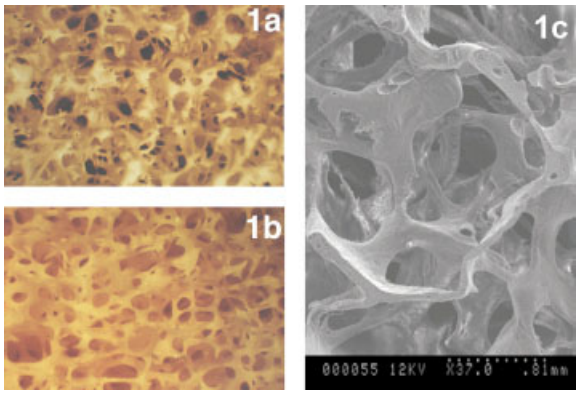

Figure 1. Light micrographs of (a) a cross-sectioned foam and (b) human trabecular bone. A similar pore structure, strut size, and distribution can be observed in both images. The overall high porosity of trabecular bone is found in the cross-sectioned scaffold (Field widths = 1.8 cm). Scanning electron micrograph of (c) a foam structure. The resemblance with trabecular bone is clearly visible. [Color figure can be viewed in the online issue, which is available at www.interscience.wiley.com.]

cellular distribution and nutrient transport throughout the scaffold, as described more fully below.

It should be emphasized that other scaffolds exhibiting similar porosity, but with a nominal pore size two orders of magnitude smaller (<10 to <100 μm) than those we describe herein, have been employed as effective hemostatic devices in which some mineralized bone-tissue islands could be identified.[1] Indeed, such bone formation is well known to occur during hematoma resolution.[17]

However, we know that scaffolds of such pore sizes would be inappropriate for a tissue-engineering strategy involving *in vitro* seeding of osteogenic cells. The early work of Rout et al.[18] clearly demonstrated that scaffolds of even 200 μm in nominal pore size would not allow cell penetration, that such pores would be overgrown by cell sheets *in vitro* and act as a barrier to cell and tissue invasion. This has been confirmed in our recent work.[19,20]

These comparisons emphasize how the biologic strategy of a proposed therapy plays a critical role in the choice of scaffold pore size and the degree of interconnected macroporosity. Indeed, the necessity for *in vitro* colonization by cells dictates a porosity that is quite different from that governing the *in vivo* response to implanted polymeric porous materials where, particularly in load-bearing conditions, it has been reported that a 200–350-μm pore-size range is optimal for invasion by host bone tissue.[21]

We prepared the scaffolds by a new process, combining phase inversion with particulate extraction. Sugar crystals were suspended in a solution of PLGA 75/25 in DMSO. The slurry was frozen and then immersed in double-distilled water (ddH_2O). The significant difference in this methodology from traditional extraction methods is the precipitation of the polymer using a phase inversion process. The latter, combined with particulate extraction, resulted in macroporous interconnectivity throughout the scaffold that previously has been unattainable. Scaffolds were characterized by both image analysis of serial thin sections with the NIH image analysis program (developed at the U.S. National Institutes of Health and available on the Internet at http://rsb.info.nih.gov/nih-image/) and mercury porosimetry. The average pore size was ≈1.44 ± 0.30 mm, with interconnections that ranged in size from 0.3 to 0.8 mm. Porosity was estimated by image analysis to be 92%, which corresponded to that measured by mercury porosimetry of 89%, notwithstanding the error associated with this technique for pores of >75 μm.[22]

After preparation, the scaffolds were rinsed extensively in ddH_2O, disinfected in 70% ethanol, rinsed with α-MEM, and then used for cell culture. We cultured Wistar rat bone marrow cells on the scaffolds using a bone-marrow cell system described previously.[13, 23] Briefly, primary marrow stromal cells were cultured for 1 week *in vitro*, collected by trypsinization, and re-seeded onto the 3-D scaffolds for an additional 6 weeks of culture. Cultures were grown in medium supplemented with dexamethasone [Dex(+)] to induce the cells to express the osteoblastic phenotype.[24–26] The control cultures were grown without dexamethasone [Dex(−)]. Bone formation was assessed by (1) osteocalcin immunolabeling with a goat anti-rat osteocalcin antibody on fixed cultures, (2) histologic observations, and (3) tetracycline labeling.

Osteocalcin easily was detected in Dex(+) cultures [Fig. 2(a)], yet only faint background immunolabeling

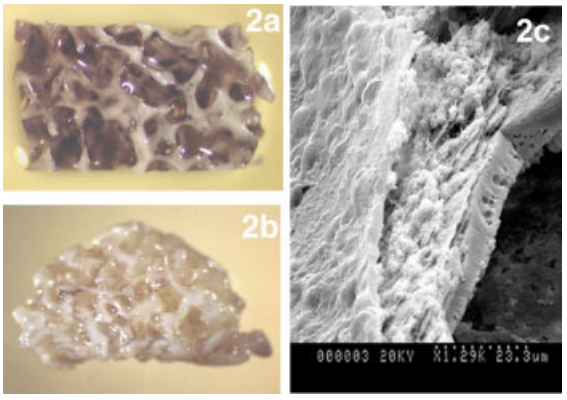

Figure 2. Light micrographs of (a) osteocalcin immunolabeled on a Dex(+) culture (field width = 1.1 cm) and (b) control sample, immunolabeled with non-immune serum. Strong immunolabeling is found on the pore walls and within the pore structure of the scaffold. Scanning electron micrograph of (c) tissue formed *in vitro* on a polymer strut within the scaffold in Dex(+) media. [Color figure can be viewed in the online issue, which is available at www.interscience.wiley.com.]

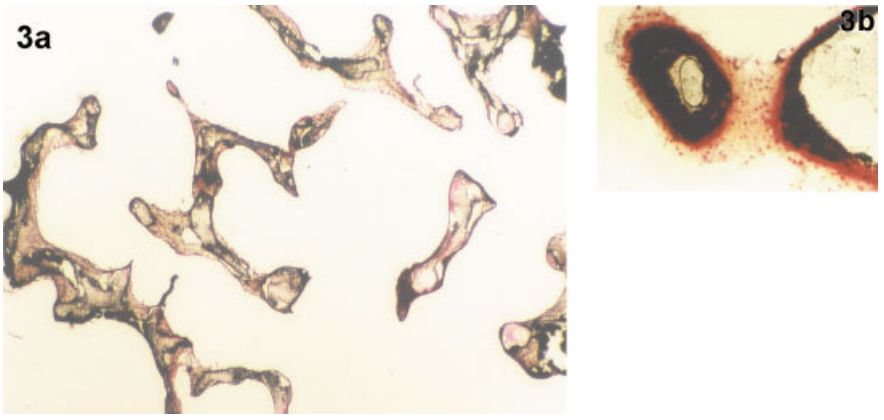

Figure 3. (a) Light micrographs of hematoxylin and eosin stained and von Kossa counterstained Dex(+) cultured scaffold sections. New tissue was found along the pore walls and throughout the entire foam section (field width = 0.8 cm); (b) detail of a hematoxylin and eosin stained nodule-like structures, as seen previously in normal bone nodule formation (field width = 558 μm). [Color figure can be viewed in the online issue, which is available at www.interscience.wiley.com.]

was observed on control samples incubated in non-immune serum [Fig. 2(b)]. While osteocalcin is considered to be the most specific marker of osteoblasts and is expressed at relatively mature differentiation stages, low levels of osteocalcin also are detectable in megakaryocytes and platelets.[27] In Dex(−) cultures, no immunolabeling was observed, confirming the specificity of the marker for mature osteoblasts (data not shown).

The lack of detectable osteocalcin labeling in Dex(−) cultures suggests that if any of these cell types survived our culture conditions, they did not contribute significantly to the positive labeling seen in our Dex(+) immunolabeled samples. The distribution and intensity of the immunolabeling on Dex(+) scaffold cultures suggests that tissue had formed throughout the entire scaffold, reflecting, of course, cellular penetration throughout the scaffold.

These results differ significantly from scaffolds prepared by salt-extraction alone, where only slight immunolabeling was visible, reflecting the presence of tissue (and thus cells) on the periphery of the scaffold (Figure not shown). The newly formed matrix also was clearly visible by scanning electron microscopy. Figure 2(c) shows a SEM photomicrograph of a Dex(+) tissue grown on a polymer strut within a scaffold. Tissue formed along the pore walls throughout the entire scaffold volume yet did not bridge across the pore interconnections. This is particularly important for 3-D tissue engineering because cell layers bridging pore interconnections may prevent nutrient and fluid flow and, ultimately, tissue growth throughout the inner volume of the construct. We believe that the latter accounts for the limited cellular penetration of cells and tissue into scaffolds prepared by salt-extraction alone.[4]

Consistent with the results from osteocalcin immunolabeling and SEM observations, cell growth throughout the entire scaffold volume was confirmed histologically with hematoxylin & eosin-stained and von Kossa-counterstained sections. A thin layer of cells lined the pore walls throughout the entire Dex(+) scaffolds [Fig. 3(a)]. Nodular structures, similar to those previously identified as bone nodules,[14] were positively labeled with von Kossa [cf. Fig. 3(b)]. While von Kossa staining has been used extensively to identify calcium phosphate deposits, it is not specific for hydroxyapatite; however, von Kossa together with the osteocalcin immunoassay suggests bone-like tissue formation.

We confirmed, in parallel experiments, that such ubiquitous bone growth did not occur in scaffolds prepared by the salt-extraction procedure alone.[9] With the latter, which exhibits a macroporous geometry but limited interconnecting macroporosity, bone grew, as previously reported, only on the outer aspects of, and not throughout, these scaffolds.[4] To the best of our knowledge, bone growth throughout such a volume has not been heretofore reported. We attribute our success in forming 3-D bone tissue to the high interconnecting macroporosity of our novel scaffolds.

Tetracycline also was used to visualize mineralized matrix deposition throughout the 3-D scaffolds *in vitro*, as has been described previously.[28–30] When tetracycline-labeled scaffolds were imaged by confocal microscopy, intense fluorescent label was again evident throughout Dex(+) cultured scaffolds.[10] At low magnification, the contours of the pore wall structures, on which cells grew and produced matrix, were clearly visible with no evidence of cells bridging the pore diameter.

To test the bone tissue engineering proof-of-principle, TECs were implanted into segmental osteotomy defect sites in New Zealand white rabbits. Defects of 1.2 cm were created in rabbit femurs that had been stabilized with titanium reconstruction plates. These defects were left empty, filled with a scaffold, or filled with a TEC seeded with autologous rabbit bone-marrow stromal cells using a cell-culture system similar to the rat-culture system described above.

As shown in a postoperative radiograph [Fig. 4(a)], the cell-loaded scaffold is radio-transparent. Postoperatively, all animals ambulated freely and were weight-bearing on the operated limb. Serial radiographs

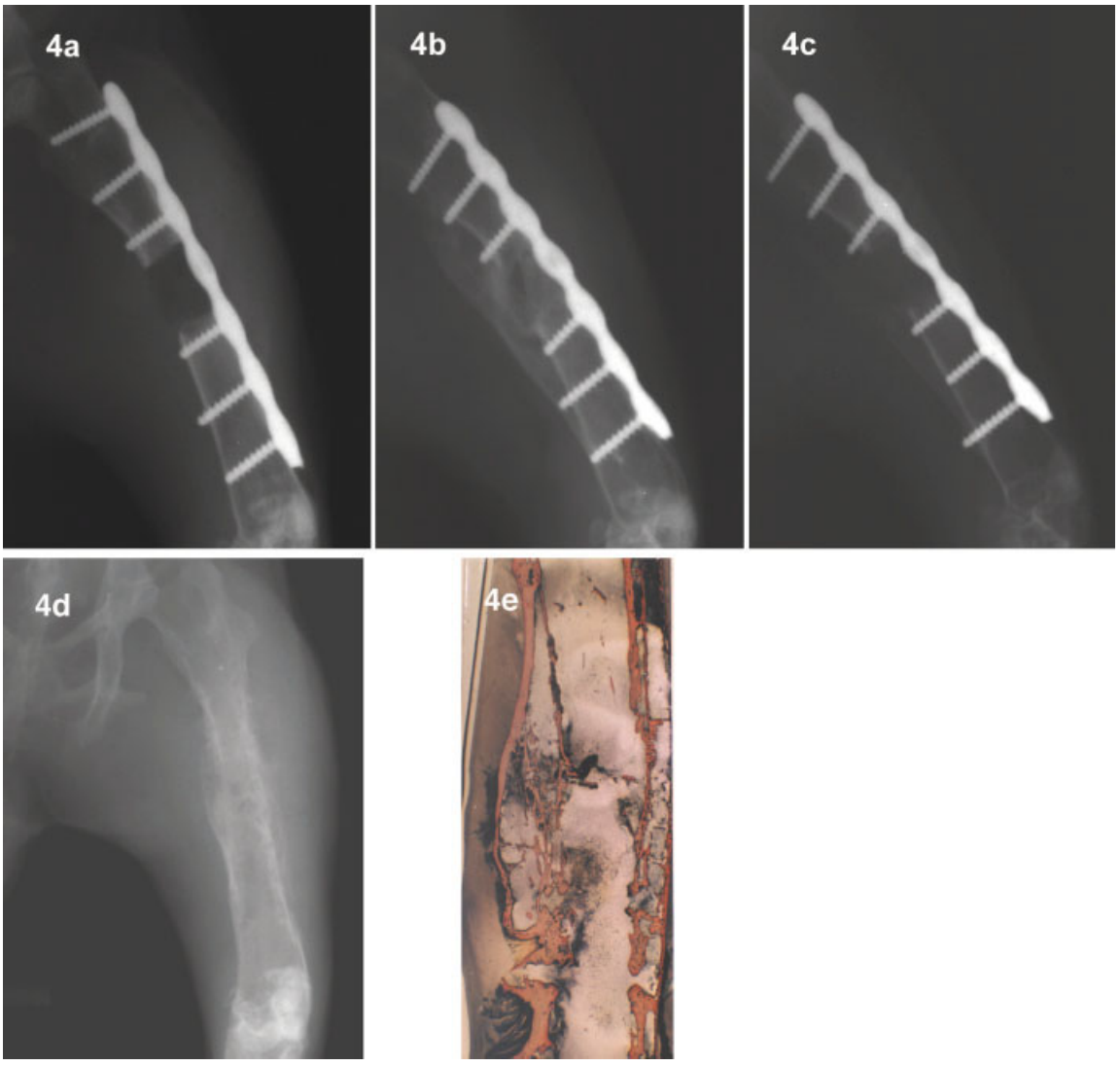

Figure 4. Radiograph, immediately post surgery, of (a) femoral segmental osteotomy performed on a 3-kg rabbit. The TEC-filled critical-size defect is radio-transparent. After 6 weeks, defects filled with TEC showed (b) radio-opacity in the defect area, indicating new bone formation throughout the osteotomy. Radiograph (c) after 6 weeks of a control defect. Eight weeks postsurgery and after removal of the plate, (d) the radio-opacity in the defect area increased relative to that observed at 6 weeks. Remodeled bone is observed histologically (e) throughout the defect after an additional 3 weeks from removal of the plate. [Color figure can be viewed in the online issue, which is available at www.interscience.wiley.com.]

showed that significantly more new bone had formed, and at earlier healing times, in the TEC group compared to the scaffold alone or to empty controls at both 2 weeks (77% for TEC, 33% for scaffold alone, and 11% for empty scaffolds) and 4 weeks (100%, 77%, and 33%, respectively). After 6 weeks, the radiographs of the TEC-filled defects indicated radio-opacity throughout the entirety of the segmental defects [Fig. 4(b)] whereas only limited radio-opacity was observed in empty [Fig. 4(c)] and scaffold-filled (figure not shown) controls.

In one case, a similar rabbit femoral defect was created and 6 weeks after implantation with a TEC, the plate was removed [Fig. 4(d)]. The animal ambulated freely for another 3 weeks, weight-bearing on the regenerated femur. The animal then was sacrificed and histology of the femur demonstrated bone union and evidence of remodeling within the defect area [Fig. 4(e)].

CONCLUSIONS

We believe that the bone tissue formation demonstrated throughout these novel 3-D scaffolds and the increase in both the rate and degree of bone regeneration in this nonunion segmental osteotomy rabbit model represent a major step forward in bone-tissue engineering. With a 3-D morphology similar to trabec-

ular bone, the biodegradable scaffolds support cell proliferation and matrix elaboration throughout their volume, thereby creating a 3-D bony structure that serves as an implant that replaces bone. We have demonstrated the *in vitro* and *in vivo* proof-of-principle required for bone-tissue engineering. In order to transfer this technology to clinical application, several unanswered questions must still be addressed. One of these is the amount of time required between cell seeding and implantation as this will directly determine the need for one procedure or two and thus affect the cost of care.

We thank Drs. J. Aubin and J.P. Vacanti for reviewing this manuscript.

References

1. Whang K, Healy KE, Elenz DR, Nam EK, Tsai DC. Engineering bone regeneration with bioabsorbable scaffolds with novel microarchitecture. Tissue Eng 1999;5:35–51.
2. Hollinger JO, Winn SR, Hu Y, Sipe R, Buck DC, Xi G. Assembling a bone-regeneration therapy. In: Davies JE, editor. Bone engineering. Toronto: em squared inc.; 2000. p 435–440.
3. Ishaug SL, Crane GM, Miller MJ, Yasko AW, Yaszemski MJ, Mikos AG. Bone formation by three-dimensional stromal osteoblast culture in biodegradable polymer scaffolds. J Biomed Mater Res 1997;36:17–28.
4. Crane GM, Ishaug SL, Mikos AG. Bone tissue engineering. Nature Med 1995;1:1322–1324.
5. Ishaug-Riley SL, Crane-Kruger GM, Yaszemski MJ, Mikos AG. Three-dimensional culture of rat calvarial osteoblasts in porous biodegradable polymers. Biomaterials 1998;19:1405–1412.
6. Lewandrowski K-U, Cattaneo MV, Gresser JD, Wise DL, White RL, Bonassar L, Trantolo DJ. Effect of a poly(propylene fumarate) foaming cement on the healing of bone defects. Tissue Eng 1999;5:305–316.
7. Ohgushi H, Caplan A. Stem cell technology and bioceramics: From cell to gene engineering. J Biomed Mater Res, Appl Biomater 1999:48:913–927.
8. Baksh D, Kim SY, Davies JE. Three dimensional matrices of calcium polyphosphates support bone growth in vitro and in vivo. J Mater Sci: Mater Med 1998;9:743–748.
9. Holy CE, Shoichet MS, Davies JE. Bone marrow cell colonization of and extracellular matrix expression on biodegradable polymers. Cells and Mater 1997;7:223–234.
10. Holy CE, Dang SM, Davies JE, Shoichet MS. In vitro degradation of a novel poly(lactide-co-glycolide) 75/25 foam. Biomaterials 1999;20:1177–1185.
11. Holy CE, Shoichet MS, Davies JE. Engineering three-dimensional bone tissue *in vitro* using biodegradable scaffolds: Investigating initial cell-seeding density and culture period. J Biomed Mater Res 2000;51:376–382.
12. Holy CE, Cheng C, Davies JE, Shoichet MS. Optimizing the sterilization of PLGA scaffolds for use in tissue engineering. Biomaterials 2001;22:25–31.
13. Davies JE. In vitro modeling of the bone/implant interface. Anat Rec 1996;245:426–445.
14. Maniatopoulos C, Sodek J, Melcher AH. Bone formation in vitro by stromal cells obtained from bone marrow of young adult rats. Cell Tissue Res 1988;254:317–330.
15. Rokkanen P, Nordstrom P, Pihlajamaki H, Toivonen T, Tormala P. Tissue response to polyglycolide and polylactide pins in cancellous bone. Arch Orthop Traumatol Surg 1998;117:197–204.
16. Rodan GA. Introduction to bone biology. Bone 1992;13:S3–S6.
17. Brighton CT, Hunt RM. Early histological and ultrastructural changes in medullary fracture callus. J Bone Joint Surg Am 1991;73:832–847.
18. Rout PGJ, Tarrant SF, Frame JW, Davies JE. Interaction between primary bone cell cultures and biomaterials. I. A comparison of dense and macroporous hydroxyapatite. In: Pizzoferrato A, Ravaglioli PG, Lee AJC, editors. Biomaterials and clinical applications. Amsterdam: Elsevier 1987;591–596.
19. Davies JE, Baksh D. Bone tissue engineering on biodegradable scaffolds. In: Tissue engineering for therapeutic use. IV. Ikada Y, Shimizu Y, editors. Amsterdam: Elsevier Science; 2000. p 15–24.
20. Baksh D, Davies JE. Design strategies for 3-dimensional in vitro bone growth in tissue-engineering scaffolds. In: Davies JE, editor. Bone engineering. Toronto: em squared inc. 2000. p 488–495.
21. Klawitter JJ, Hulbert SF. Application of porous ceramics for the attachment of load-bearing orthopedic applications. J Biomed Mater Res Symp 1971;2:161–168.
22. Schugens C, Maquet V, Grandfils C, Jerome R, Teyssie P. Polylactide macroporous biodegradable implants for cell transplantation. II. Preparation of polylactide foams by liquid–liquid phase separation. J Biomed Mater Res 1996;30:449–461.
23. Davies JE, Chernecky R, Lowenberg B, Shiga A. Deposition and resorption of calcified matrix in vitro by rat bone marrow cells. Cells and Mater 1991;1:3–15.
24. Rodan GA, Martin TJ. Role of osteoblasts in hormonal control of bone resorption—A hypothesis. Calcif Tissue Int 1981;33:349–351.
25. Bellows CG, Aubin JE, Heersche JNM, Physiological concentrations of glucocorticoids stimulate formation of bone nodules from isolated rat calvaria cells in vitro. Endocrinology 1987;121:1985–1992.
26. Cheng SL, Yang JW, Rifas L, Zhang SF, Avioli LV. Differentiation of human bone marrow osteogenic stromal cells in vitro: Induction of the osteoblast phenotype by dexamethasone. Endocrinology 1994;134:277–286.
27. Thiede MA, Smock SL, Petersen DN, Grasser WA, Thompson DD, Nishimoto SK. Presence of messenger ribonucleic acid encoding osteocalcin, a marker of bone turnover in bone marrow megakaryocytes and peripheral blood platelets. Endocrinology 1994;135:929–937.
28. Lian JB, Stein GS. Concepts of osteoblast growth and differentiation: Basis for modulation of bone cell development and tissue formation. Crit Rev Oral Biol Med 1992;3:269–305.
29. Bradbeer JN, Zanelli JM, Lindsay PC, Pearson J, Reeve J. Relationship between the location of osteoblastic alkaline phosphatase activity and bone formation in human iliac crest bone. J Bone Miner Res 1992;7:905–912.
30. Chentoufi J, Hott M, Lamblin D, Buc-Caron MH, Marie PJ, Kellermann O. Kinetics of in vitro mineralization by an osteogenic clonal cell line (C1) derived from mouse teratocarcinoma. Differentiation 1993;53:181–189.